Robotica: (2021) volume 39, pp. 652–664. © The Author(s), 2020. Published by Cambridge University Press.
doi:10.1017/S0263574720000648

A Human Arm's Mechanical Impedance Tuning Method for Improving the Stability of Haptic Rendering

Xiong Lu*, Beibei Qi, Hao Zhao and Junbin Sun

College of Automation Engineering, Nanjing University of Aeronautics and Astronautics, Nanjing 211106, China

(Accepted June 19, 2020. First published online: July 21, 2020)

SUMMARY

Rendering of rigid objects with high stiffness while guaranteeing system stability remains a major and challenging issue in haptics. Being a part of the haptic system, the behavior of human operators, represented as the mechanical impedance of arm, has an inevitable influence on system performance. This paper first verified that the human arm impedance can unconsciously be modified through imposing background forces and resist unstable motions arising from external disturbance forces. Then, a reliable impedance tuning (IT) method for improving the stability and performance of haptic systems is proposed, which tunes human arm impedance by superimposing a position-based background force over the traditional haptic workspace. Moreover, an adaptive IT algorithm, adjusting the maximum background force based on the velocity of the human arm, is proposed to achieve a reasonable trade-off between system stability and transparency. Based on a three-degrees-of-freedom haptic device, maximum achievable stiffness and transparency grading experiments are carried out with 12 subjects, which verify the efficacy and advantage of the proposed method.

KEYWORDS: Haptic rendering; System stability; Impedance tuning; Magnetic field; Mechanical impedance; Maximum achievable stiffness.

1. Introduction

Haptic feedback can provide kinesthetic or tactile information about virtual objects in virtual environments, which in turn can offer higher levels of immersion and realism. In addition to enhancing the application of virtual reality systems in traditional fields, haptic rendering further expands other application areas of virtual reality, such as surgery training,[1,2] virtual prototyping,[3] and scientific visualization.[4] Interaction stability is the premise for modeling and simulating in haptic rendering systems and ensuring high performance and fidelity during the haptic rendering process. Some factors contribute to system instability (especially for rendering rigid objects), including position sensor quantization, time delay, update rate, and in particular the dynamics of the human arm, and these "non-idealities" will cause energy leakages. System instability will not only reduce the performance of haptic rendering systems but also may damage the hardware equipment and even hurt the human operator. Therefore, improving the stability of the haptic rendering system is a significant challenge.

Since the behavioral characteristics of operators are generally complex and difficult to describe with a common model, considerable researchers have studied the stability of haptic systems from the perspective of passivity. Colgate et al.[5–7] have employed passivity theory to derive a stability condition on virtual wall stiffness and developed the virtual coupling to guarantee system stability. They proposed the formula for the stability of the system in the virtual wall model:[8]

$$\mathrm{b} > KT/2 + B \tag{1}$$

* Corresponding author. E-mail: luxiong@nuaa.edu.cn

Here, b and B are the damping coefficients of equipment and virtual wall, respectively. K is the virtual wall stiffness, while T is the force update period. They suggested that the "active" nature of virtual walls can lead to instability of haptic rendering, which is more intense at the moment of the collision. Hu et al.[9] proposed a maximum output force controller based on passive theory to achieve stable interactions with high transparency. A novel criterion method was proposed by Mendez et al.[10] to analyze the stability of multilateral haptic systems based on passivity. A new criterion for the passivity of haptic devices was obtained in Ref. [11], which created a relationship between the Coulomb friction coefficient, viscous friction coefficient, sampling rate, and the maximum simulated stiffness. It is well known that friction in haptic devices plays a key role in dissipating surplus energy to maintain the passivity of the haptic system. So the Coulomb friction component in Refs. [12, 13] was taken into account in force bounding approach which stabilized haptic interaction through reducing energy accumulation.

Stability boundary methods have also been proposed for haptic systems. Park et al.[14] proposed an energy bounding approach (EBA) for improving the transparency where passivity based on EBA can guarantee the stability of haptic interaction systems. A stability criterion was developed by Mashayekhi et al.[15] to predict the stability boundaries, especially without restrictions on time delay and virtual damping. In Ref. [16], the stability boundary has been extended through a method of high-impedance actuator fusion. There are also several approaches aiming to enhance system stability. Compared with the passivity-based control approach, the input-to-state stable approach[17] was less conservative which can increase the maximum apparent impedance. A new approach was proposed in Ref. [18] with a dual-rate sampling scheme, which can stably increase the stiffness range of a virtual wall. There was an impedance-type force-feedback architecture using linear matrix inequality (LMI) to improve the stability of haptic systems.[19] Similarly, Liu et al.[20] proposed a stability criterion based on LMI to obtain stable haptic systems. A local stiffness matrix is constructed to compute feedback force at a higher update rate for interaction with deformable objects, which removes the trade-off problem of conventional haptic rendering between the stability and performance.[21] Moreover, several controllers and observers are utilized to improve the stabilities of haptic systems. A time-domain vibration observer and controller were studied to reduce vibration that may destroy the performance in interactions.[22] Aydin et al.[23] proposed a fractional order admittance controller aiming at generating stable and realistic haptic feedback. Lu and Song[24] presented an energy-compensating controller to improve system stability and achieve a more realistic perception of rigid objects through compensating for the energy flows both out of and into the haptic system. Amirkhani et al.[25] have used an energy-compensating controller to eliminate energy leakage, while a fuzzy impedance controller was utilized to control position.

However, some researchers have considered the existence of the operator's behavior and analyzed its influence on system stability conditions.[26] Burdet et al.[27] examined arm movements in an unstable dynamic environment created by a robotic interface. Their results showed that humans learn to stabilize unstable dynamics using the skillful and energy-efficient strategy of selective control of impedance geometry. In human activities, many motor behaviors may have been used to regulate their limb mechanics and to provide stability during interactions with destabilizing environments. The dynamics of the human arm were modeled as mechanical impedance in Ref. [28]. A second-order mass-damper-spring system was used to model the human arm impedance in Ref. [29], where the maximum achievable stiffness of haptic systems was increased based on the value of human arm impedance. It was explicitly studied in Ref. [26] that human arm impedance modeling can improve the stability and transparency of haptic systems. Studies showed that mechanical impedance of the human arm depends on arm posture,[30] force applied on the hand (the degree of muscle activation),[31] and environmental instability.[32,33] Impedance was related to muscle activation so that an important characteristic of the neuromuscular system was control of mechanical impedance.[34] Also, a reliable estimation method was proposed in Ref. [35] to estimate the arm mechanical impedance without force or acceleration sensors. Piovesan et al. investigated the mechanical changes of the arm when completing the force control task during low-frequency positional perturbations of the arm.[36] They concluded that humans use predictive internal models to construct trajectories and modulate their impedance, increasing it over time. For upper limb rehabilitation, Song et al. proposed a mechanical impedance identification method for human arm and rehabilitation robotic.[37] The identification results of the arm mechanical impedance were utilized to adjust the control parameters of the mechanical arm, thereby achieving stable human–machine interaction control.

https://doi.org/10.1017/S0263574720000648 Published online by Cambridge University Press

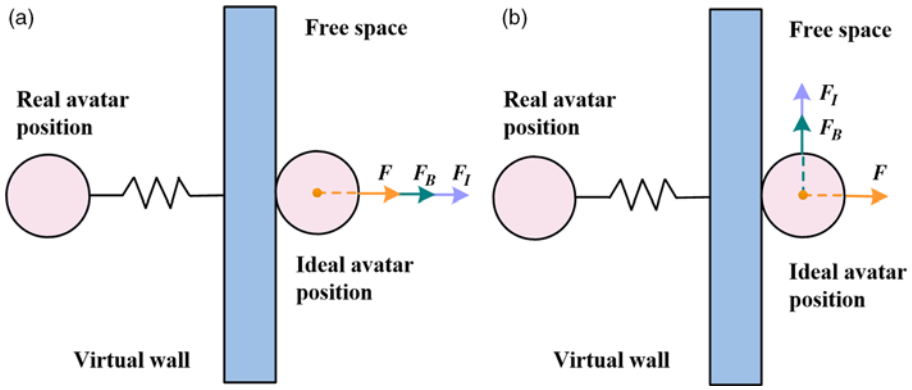

Fig. 1. Virtual wall model with background force fields. (a) The interference force is perpendicular to the virtual wall surface. (b) The interference force is parallel to the virtual wall surface.

Considering the adjustable characteristics of the mechanical impedance of human arms, we have carried out preliminary works of tuning the mechanical impedance of the human arm by superimposing the magnetic field to improve system stability[38] and subsequently carried out experimental research to verify that the human arm impedance can suppress the externally applied interference.[39] This paper systematically demonstrates the influence of arm's mechanical impedance on the system stability and then proposes a method to improve haptic stability through tuning arm's mechanical impedance.

The remaining of this paper is organized as follows. Section 2 presents the external force disturbance experiments to prove that arm mechanical impedance can be modified unconsciously to stabilize unstable motions. The proposed impedance tuning (IT) method and an adaptive impedance tuning (AIT) method are presented in Section 3. Section 4 describes experiments designed to evaluate the IT and AIT methods. The experimental results and issues are drawn in Section 5. Conclusions and future works are summarized in Section 6.

2. Influence of the Human Arm Impedance on Unstable Motions

The dynamic characteristics of an operator's arm during haptic rendering can be described with mechanical impedance, which stems from the circuit impedance and is used to describe the relationship between force and displacement. Several factors will determine the change of mechanical impedance, such as position, muscle activation degree, and the stability of the interaction. And researches have shown that general characteristics of the human arm's mechanical impedance include individual-based variation, direction-based variation, and the ability to regulate values during interactions.

In this section, experiments of haptic interaction were carried out to verify the human's ability to address disturbances through impedance regulation. To tune the mechanical impedance of the operator's arm, two kinds of interference models were designed with external disturbance forces, where background forces are imposed for modifying arm impedance. Subjects were asked to control the haptic device to conduct a series of interactions with a virtual wall.

2.1. Virtual wall model with interference force

2.1.1. Perpendicular interference force. We assume that the avatar moves along the x-axis and the virtual wall is described with $x < x_w$. As the avatar interacts with the wall, a feedback force F will be exerted on the avatar. The model in Fig. 1(a) gives the avatar a jitter during its contact with the virtual wall, where interference force F_I is perpendicular to the virtual wall. A background force F_B is added to tune the mechanical impedance of the human arm. This model is given by

$$\widehat{\mathrm{F}} = \begin{cases} F_B, & \mathrm{x} > x_w \\ F + F_B + F_I, & \mathrm{x} \leq x_w \end{cases} \tag{2}$$

https://doi.org/10.1017/S0263574720000648 Published online by Cambridge University Press

Table I. The average jitter amplitude and the adjustment time under different interference and background forces.

	The average jitter amplitude of six subjects (*Jit*/0.1 mm)/the average adjustment time of six subjects (*AT*/ms)			
$F_B(N)$ /$F_I(N)$	**1.0**	**3.0**	**5.0**	**7.0**
0.0	0.0/0.0	40.0/75.0	60.0/120.0	100.0/195.0
1.0	0.0/0.0	30.0/60.0	40.0/90.0	90.0/165.0
2.0	NA[a]	16.0/45.0	30.0/120.0	60.0/105.0
3.0	NA	30.0/60.0	40.0/90.0	60.0/90.0
4.0	NA	NA	36.0/75.0	50.0/90.0

[a]To guarantee system transparency, the value of F_B is always less than F_I. NA represents Not Available.

where x is the position of avatar, x_w is the position of the virtual wall, and F is the generated interacting force with the simple spring model, which is defined as

$$\mathrm{F} = \begin{cases} 0, & \mathrm{x} > x_w \\ K(x_w - x), & \mathrm{x} \le x_w \end{cases} \tag{3}$$

where K is the stiffness of the virtual wall.

2.1.2. Parallel interference force. We set an interference force F_I parallel to the virtual wall but perpendicular to the moving direction of the avatar in Fig. 1(b). Also, a background force F_B is added in this space to tune the mechanical impedance of the human arm. The model is given by

$$\widehat{\mathrm{F}} = \begin{cases} 0, & \mathrm{x} > x_w \\ F + F_I, & (\mathrm{x} \le x_w)\ \&\&(\mathrm{t} < t_0) \\ \mathrm{F} + \mathrm{F}_I + \mathrm{F}_B, & (\mathrm{x} \le x_w)\ \&\&(\mathrm{t} \ge t_0) \end{cases} \tag{4}$$

2.2. Comparative experiments

Six volunteers (four males and two females, aging from 22 to 25) took part in the experiments. Experiments verify the capability of operators for restraining the external interference in different situations.

2.2.1. Perpendicular interference force. Six subjects were instructed to control the avatar to touch against the virtual wall in this experiment, while the external interference force perpendicular to the virtual wall surface was imposed. *Jit* denotes the average amplitude of the jitter and AT refers to the adjustment time needed for subjects to recover from the interference disturbance. In Fig. 2, the interference force is 5.00 N and the background force is 3.00 N. The results show that both AT and *Jit* decrease significantly when background force is added, which means that effects caused by the interference force have been reduced.

Then, experiments with different values of interference forces and background forces were carried out. Table I shows that *Jit* and AT decrease when F_B increases. However, there should be an upper limit for F_B because an oversized value of F_B may distort fidelity and transparency of free space in haptic rendering.

2.2.2. Parallel interference force. In this experiment, operators were instructed to keep the avatar stable against the virtual wall, with interference forces parallel to the surface of virtual wall. *Dev* denotes the position deviation caused by the interference force.

In Fig. 3, the first five pulses show experimental results of the external interference force of 5.00 N without the background force, and the last five pulses show experimental results with a background force of 3.00 N. It is shown that *Dev* decreases dramatically with the existence of the background force, which is believed to have increased the mechanical impedance of the human arm to restrain the external interference during the experiment.

https://doi.org/10.1017/S0263574720000648 Published online by Cambridge University Press

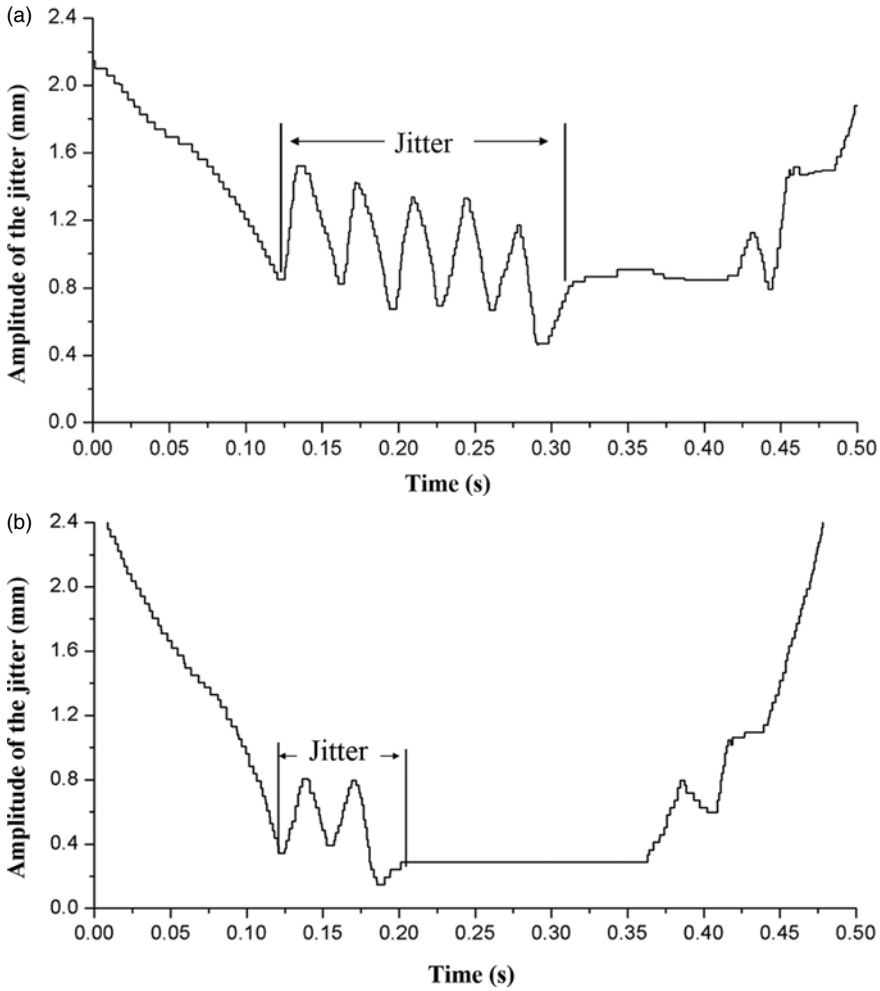

Fig. 2. Jitter caused by interference force. (a) Jitter without background force field. (b) Jitter with a background force field.

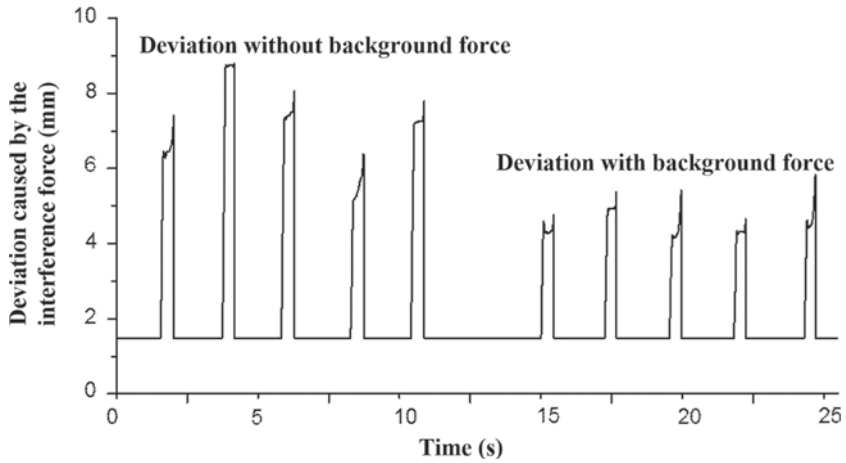

Fig. 3. Position deviation due to external interference force (5.00 N) parallel to the virtual wall's surface, without and with the background force (3.00 N).

https://doi.org/10.1017/S0263574720000648 Published online by Cambridge University Press

Table II. Position deviation caused by different interference and background forces.

	The average deviation of six subjects (*Dev*/0.1 mm)			
$F_B(N)/F_I(N)$	**1.0**	**3.0**	**5.0**	**7.0**
0.0	0.0	14.0	94.0	166.0
1.0	0.0	10.2	76.0	150.0
2.0	NA[a]	8.6	44.0	110.0
3.0	NA	6.8	36.0	92.0
4.0	NA	NA	24.0	78.0

[a]To improve system transparency, the value of F_B is always less than F_I. NA represents Not Available.

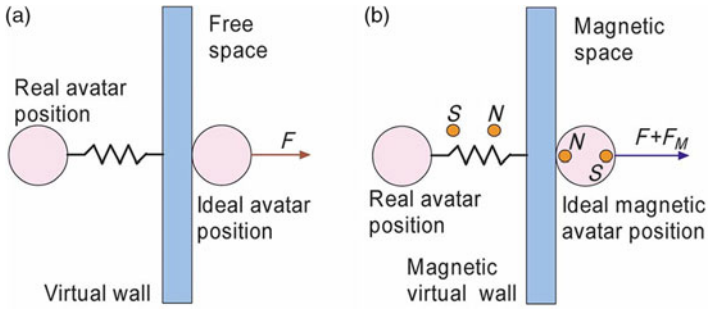

Fig. 4. Virtual wall model: (a) plain virtual wall and (b) magnetic virtual wall.

Experiments with different values of interference forces and background forces have been carried out. Results in Table II show that the average deviation decreases while the background force increases.

From these experimental results, it can be found that a larger background force will lead to a stronger ability for inhibiting external disturbances because the background force may change the mechanical impedance of the human arm.

3. The Haptic Rendering Method Through Tuning the Operator's Arm Mechanical Impedance

From the above experiments, it can be concluded that background force increases the mechanical impedance of the human arm, which has the potential for improving the stability of haptic rendering systems. Based on this inspiration, we proposed the IT method and AIT algorithm for tuning the mechanical impedance.

3.1. System models

In the haptic rendering system, the stability of the interaction is the coupling stability including the human operator. When the stiffness coefficient of a virtual object is high, some non-ideal factors will lead to energy leaks and cause system instability in haptic rendering. Therefore, unlike its counterpart in the real world, the virtual wall will be non-passive and output additional energy to the operator, who touches it through a haptic device. In this paper, we proposed to apply additional forces to the human arm for gradually tuning the mechanical impedance to improve system stability.

For applying force to change the muscle activation of the human operator, a magnetic virtual wall model is proposed. Figure 4 (b) shows the model of a magnetic virtual wall, while Fig. 4 (a) shows that of a plain virtual wall. In Fig. 4 (b), an ideal magnetic field is imposed on the plain virtual wall and a magnetic avatar is used to represent the haptic device. The magnetic avatar is set to always repels from the magnetic wall, and a repulsive magnetic force existing between them is

$$F_M = \begin{cases} \dfrac{F_{MC}}{(|x_x - x|/x_0 + 1)^2}, & x > x_w \\ F_{MC}, & x \le x_w \end{cases} \tag{5}$$

https://doi.org/10.1017/S0263574720000648 Published online by Cambridge University Press

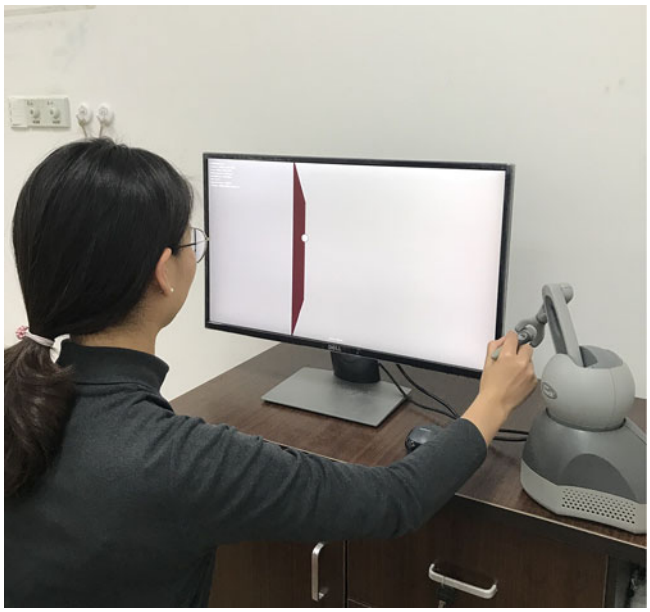

Fig. 5. System configuration.

where F_{MC} is the magnetic coefficient for adjusting the intensity of the magnetic field and x_0 is a specified displacement constant such as 1.0 mm. The interaction force in the virtual magnetic wall model with the spring model is obtained as

$$\widehat{\mathrm{F}} = \begin{cases} \dfrac{F_{MC}}{(|x_w - x|/x_0 + 1)^2}, & x > x_w \\ K_W(x_W - x) + F_{MC}, & x \le x_w \end{cases} \tag{6}$$

When the avatar is far away from the magnetic wall, magnetic force F_M is very small (approaching zero) just like in the free space (Fig. 4(a)). As the avatar approaches the magnetic wall, the magnetic force F_M gradually increases to F_{MC} and keeps the value of F_{MC} during interacting with the magnetic wall.

4. Experiments and Results

To validate the IT method, we carried out experiments with a Geomagic Touch (formerly Sensable Phantom Omni) (3D Systems Inc. Rock Hill SC, USA) haptic device (the workspace $>$ 160 W $\times$ 120 H $\times$ 70D mm; position resolution 0.055 mm; the maximum output force 3.3 N) for comparing the performance of the plain virtual wall model and the magnetic virtual wall model, as shown in Fig. 5.

4.1. Experiment step

Twelve normal volunteers (seven males and five females) participated in the experiment, aging from 23 to 26. Each subject was provided with a warm-up period to get familiar with the haptic device. Then, each subject was asked to make contact with the plain virtual wall and magnetic virtual wall, respectively, which includes the pushing, holding, and releasing the haptic device. The stability and performance of two haptic systems with the IT method (magnetic virtual wall) and without the IT method (plain virtual wall) were compared with each other.

4.2. Experiments with constant magnetic coefficients F_{MC}

This experiment is mainly used to measure the maximum achievable stiffness $K_{\max}$ of the system with the IT method in the magnetic virtual wall model. $K_{\max}$ is defined as the maximum stiffness coefficient used for simulating the virtual wall under the premise that subjects cannot cause the system to be unstable. To examine the effect of the IT method, the magnetic coefficient F_{MC} was set to 0.00 N (i.e., the plain virtual wall), 0.50 N, 1.00 N, 1.50 N, and 2.00 N respectively. The adjusting

https://doi.org/10.1017/S0263574720000648 Published online by Cambridge University Press

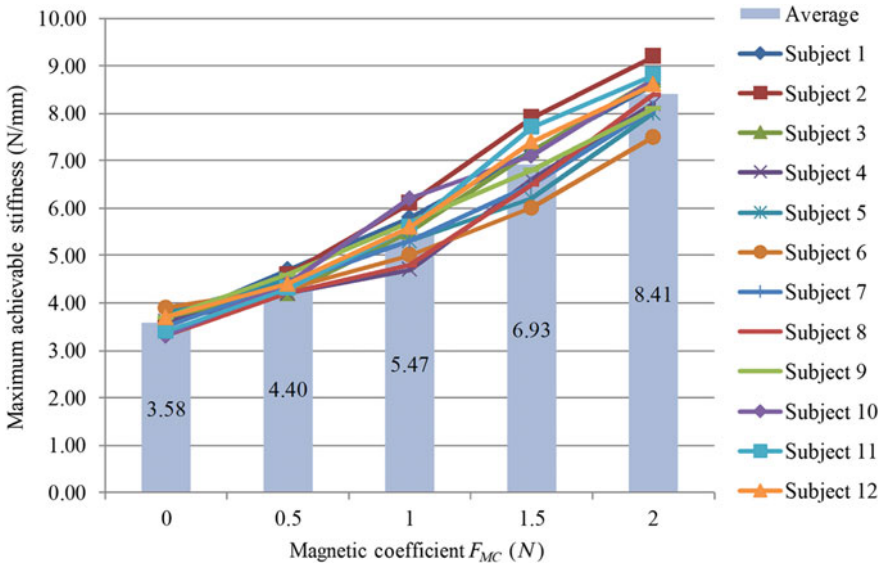

Fig. 6. Maximum achievable stiffness for plain virtual wall and magnetic virtual wall in the IT method.

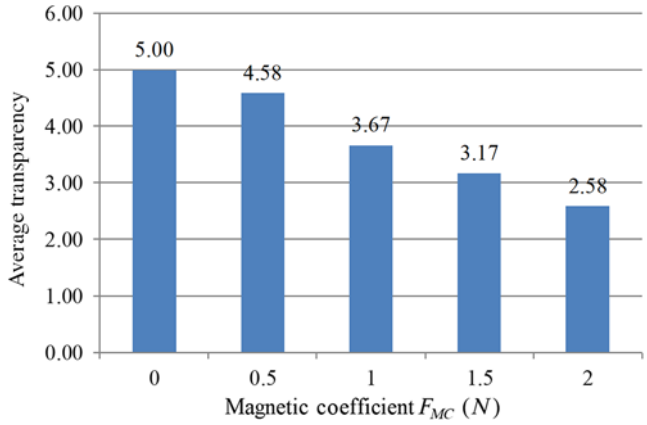

Fig. 7. Average transparency rating of magnetic virtual walls (IT method) with 12 subjects.

step of the stiffness coefficient of the magnetic virtual wall is 0.10 N/mm with the initial value of 3.00 N/mm. The force update rate K_S was set to 500 Hz. When each $K_{\max}$ was achieved, the subject was asked to evaluate the transparency of the current haptic system, by rating the transparency with a number between 0 (lowest transparency) and 5 (highest transparency). The transparency of the plain virtual wall is specified as 5, while 0 represents the system with the worst transparency. The excessive magnetic force will reduce the transparency of the system because the subjects will feel the repulsive background force when the avatar moves to approach the surface of the virtual wall. The experimental results with $K_{\max}$ and average transparency are shown in Figs. 6 and 7, respectively.

The data in Fig. 6 show that the IT method can effectively improve the maximum achievable stiffness $K_{\max}$. Compared with the plain virtual model with the average $K_{\max}$ of 3.58 N/mm, the average value $K_{\max}$ of 8.41 N/mm can be achieved for the magnetic virtual model with the F_{MC} being 2.00 N, leading to a prominent improvement of nearly 140%. However, Fig. 7 shows that the greater the magnetic force applied to the system, the lower the system transparency will be.

4.3. Experiments with adaptive magnetic coefficients F_{MC}

To further reduce the influence of imposed magnetic force on system transparency while guaranteeing system stability, we propose an AIT algorithm, in which the magnetic coefficient varies according to the velocity of the human arm (hand). Three basic functions of the human arm's velocity V, i.e.,

https://doi.org/10.1017/S0263574720000648 Published online by Cambridge University Press

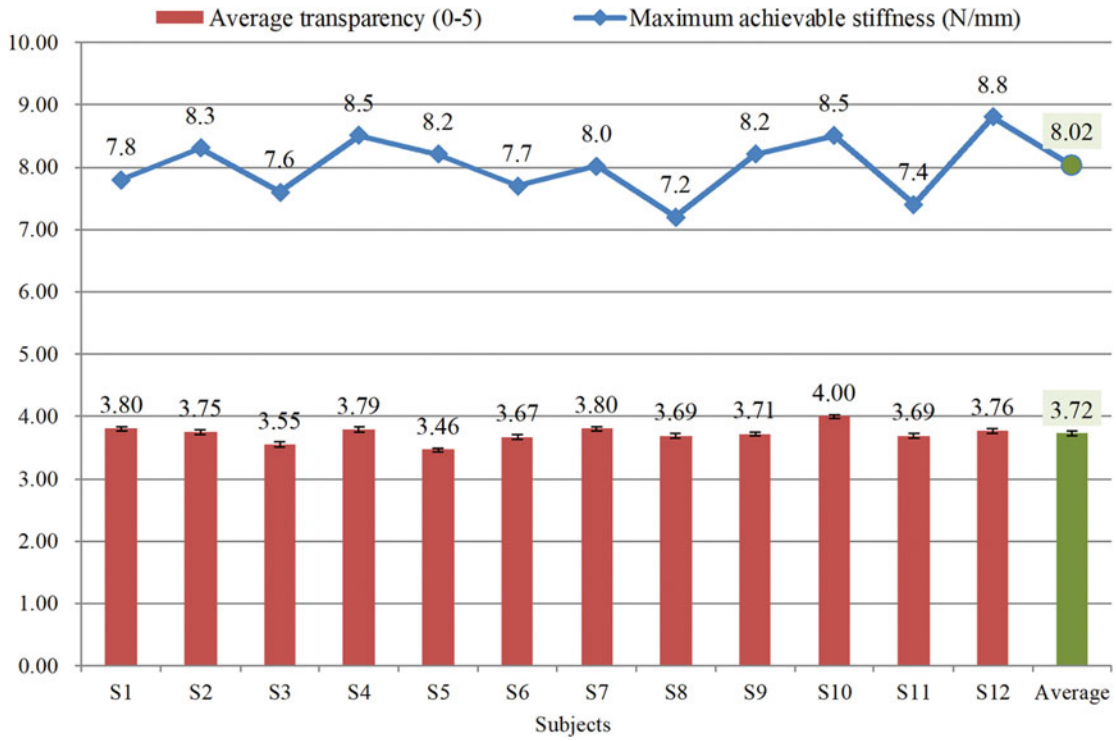

Fig. 8. Maximum achievable stiffness K_{max} and average transparency ratings for 12 subjects in the AIT method.

avatar's velocity, are proposed to define the value of the magnetic coefficient F_{MC} in equation (6), which are linear relationship, square relationship, and square root relationship, respectively. Through comparative experimental trials, we found that the [0.8 N, 2.0 N] is the best interval for F_{MC}. Then, a linear relationship between the magnetic coefficient and the velocity of the human arm was chosen in our AIT method as

$$F_{MC} = 2.4\mathrm{V_k} + 0.8, \quad V_k = V / V_{max} \tag{7}$$

where $V_{\max}$ is the maximum velocity of the human hand which controls the avatar to move toward the virtual wall, and its value is set to 2.4 m/s in our method. The velocity coefficient V_k is used to normalize the velocity of the human hand, which is defined as the ratio of the current velocity V to $V_{\max}$.

During the experiment of our proposed AIT method, the stiffness coefficient K_W of the magnetic virtual wall was set to the initial value of 5.00 N/mm and adjusted with a step of 0.10 N/mm. Each subject was asked to contact with the magnetic virtual wall at any velocity and rate the system transparency of each situation until the maximum achievable stiffness $K_{\max}$ was obtained. The experiment results of $K_{\max}$ and the average transparency rating scores of each subject in the AIT method are given in Fig. 8.

The experiment results in Fig. 8 show that the proposed AIT method can lead to large values of maximum achievable stiffness $K_{\max}$ (with the average value of 8.02 N/mm) while at the same time guarantees system transparency (with the average value of 3.72) by adaptively adjusting the magnetic coefficient F_{MC} according to the velocity of the human arm, compared with the IT method with the magnetic coefficient F_{MC} being constant (for $F_{MC} = 2.00$ N, the average $K_{\max}$ and transparency are 8.41 N/mm and 2.58, respectively). Therefore, the AIT method performs better than the IT method in general situations where the operators can interact with the virtual wall at any free velocity.

4.4. Performance comparison of systems with IT method and AIT method

This experiment compares the performance of magnetic virtual walls implemented with the IT method for three different magnetic coefficient F_{MC} values of 0.00 N, 1.00 N, and 2.00 N, and the magnetic virtual wall with the AIT method. The stiffness K_W for each magnetic virtual was

https://doi.org/10.1017/S0263574720000648 Published online by Cambridge University Press

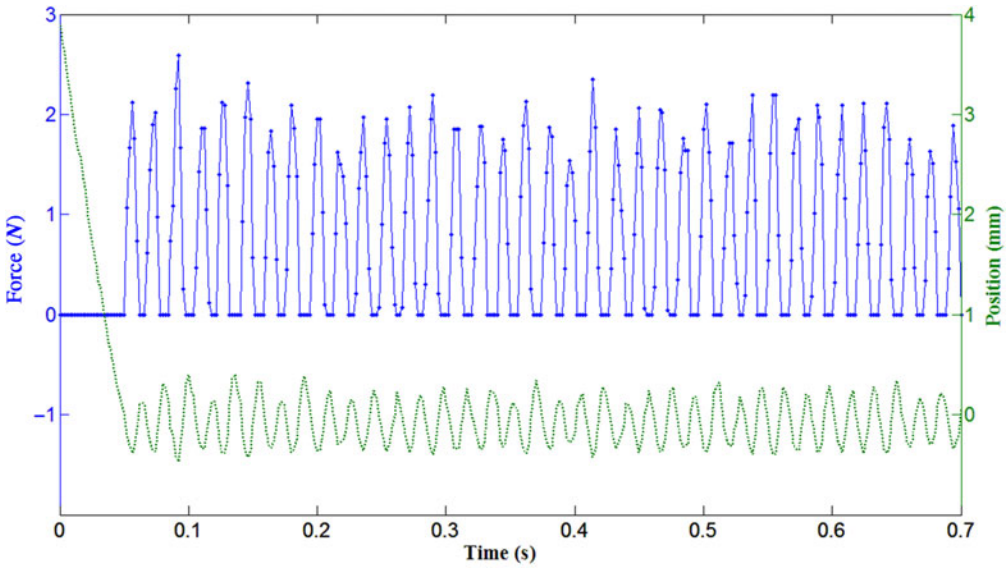

Fig. 9. Operator interacting with the virtual wall in the IT method ($F_{MC} = 0.00N$).

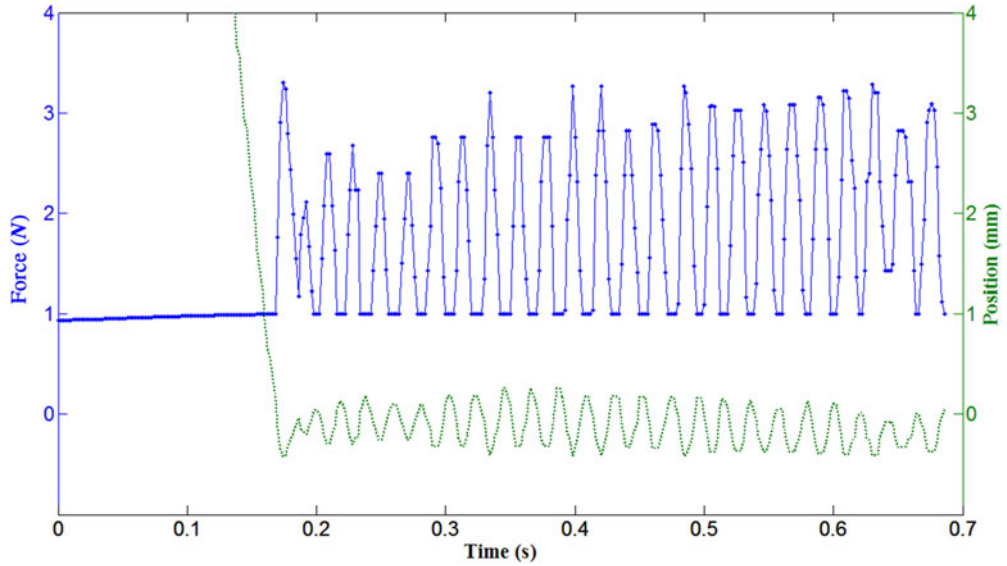

Fig. 10. Operator interacting with the virtual wall in the IT method ($F_{MC} = 1.00N$).

set to 5.50 N/mm and the force update rate K_S was set to 500 Hz. The results of Subject No. 1 in the IT method with different F_{MC} values of 0.00 N, 1.00 N, and 2.00 N are shown in Figs. 9–11, respectively. And Fig. 12 shows the results of the same Subject No. 1 in the AIT method.

When F_{MC} was 0.0 N, the magnetic virtual wall turned to a plain virtual wall and became unstable with the high stiffness of 5.50 N/mm, where disturbing oscillations with large magnitudes seriously degraded the fidelity of haptic simulation for the virtual wall (Fig. 9). For the magnetic virtual wall in the IT method with F_{MC} being set to 1.00 N, although the tuned impedance of the subject's arm was not sufficient to restrain the instability, a decrease of the magnitude of disturbing oscillation can be achieved, as shown in Fig. 10. When F_{MC} was set to 2.00 N, the mechanical impedance of the subject's arm was tuned to stabilize the haptic interaction sufficiently (Fig. 11). The data in Fig. 12 show that the magnetic virtual wall with the AIT method also leads to a stable haptic rendering with the advantage of an adaptively adjusting magnetic coefficient F_{MC}, which guarantees the performance of system transparency.

https://doi.org/10.1017/S0263574720000648 Published online by Cambridge University Press

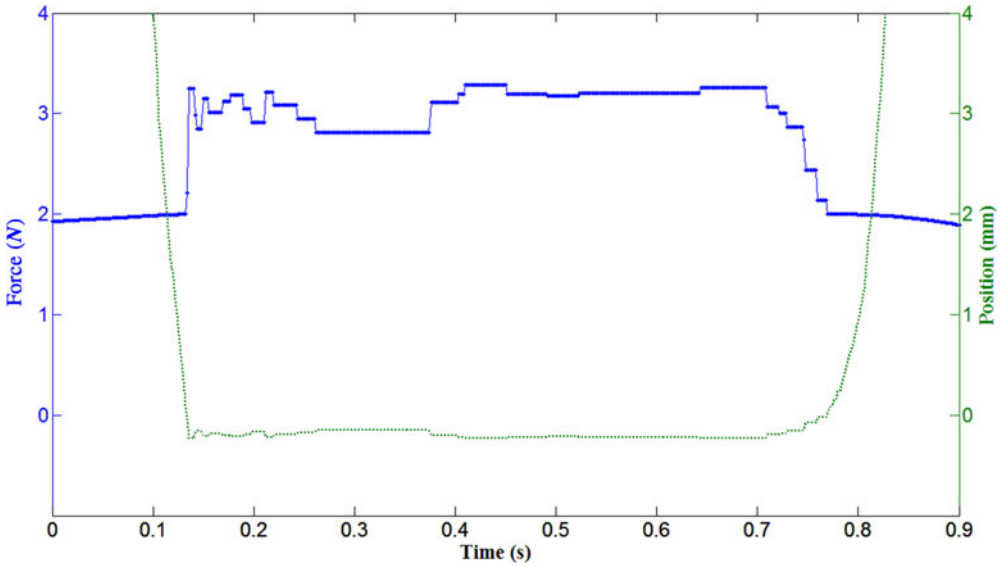

Fig. 11. Operator interacting with the virtual wall in the IT method ($F_{MC} = 2.00\ N$).

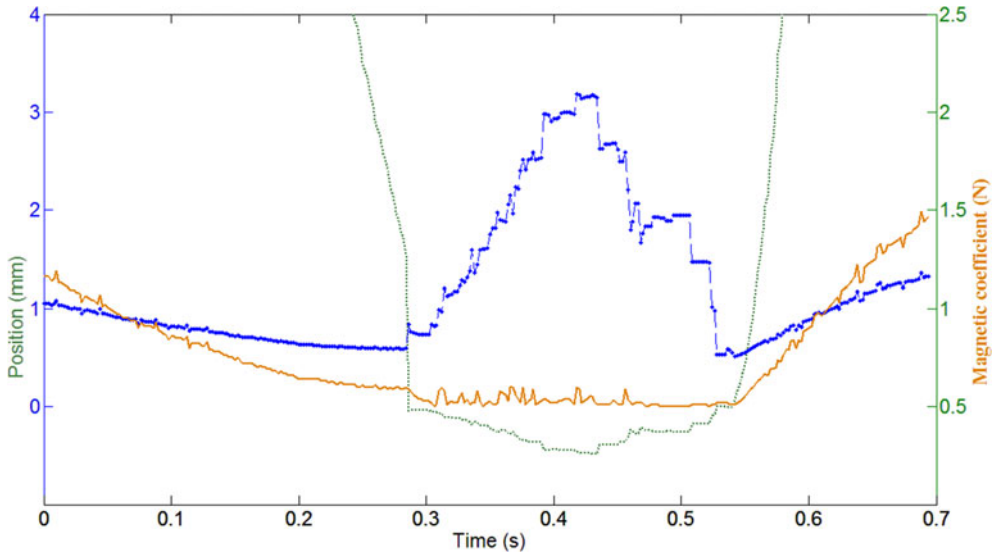

Fig. 12. Operator interacting with the virtual wall in the AIT method.

5. Discussions

Because of the inherent characteristic of a sampled-data system and several inevitable "non-idealities" in the system, a haptic rendering system may be unstable, especially when rendering virtual objects under large stiffness values. A considerable number of researchers have addressed the stability problem of haptic rendering based on the concept of system passivity. However, it is confirmed that the passivity-theory-based methods or absolute stability criteria are generally conservative, which do not take the importance and role of the human operator into consideration. Because the behavioral characteristics of operators are complicated, it is difficult to describe them comprehensively with a single general model. Mechanical impedance is the relationship between the net force applied on a mechanical system and the system's resulting kinematics, that is, position, velocity, and acceleration. Experimental studies have demonstrated that the mechanical impedance of the human arm can vary over a wide range. Although it will take at least 1.2–1.5 seconds for the mechanical impedance of a human arm to be adjusted,[40] it can effectively suppress external disturbances, such as instability, during interacting with the environment.[27]

https://doi.org/10.1017/S0263574720000648 Published online by Cambridge University Press

In this paper, taking into account the influence of the human operator on the performance of haptic systems, we proposed an IT method for haptic rendering, which uses a gradually position-based force field to regulate the arm mechanical impedance just before the human operator interacts with stiffness objects. This superimposed force field over traditional haptic rendering will increase the human operator's muscle activation, improve its ability to address uncertain external disturbance, and contribute to the improved system stability. Furthermore, the proposed AIT algorithm regulates the mechanical impedance of the human arm with an adaptive magnetic force related to the human arm's velocity. In this way, the AIT method effectively guarantees better system transparency, compared with the IT method. Therefore, the AIT method can significantly improve the stability of the system and guarantee system transparency at the same time.

6. Conclusions and Future Works

Based on the variability of the mechanical impedance of the human arm, we propose an IT method to regulate the mechanical impedance of the human arm through superimposing an ideal magnetic field to the traditional haptic system, which improves the human arm's ability for suppressing possible disturbance and leads to stable haptic rendering, even for rendering rigid objects with large stiffness values. Furthermore, an AIT algorithm has been proposed to improve system stability without the sacrifice of system transparency by adjusting the maximum magnetic force according to the velocity of the human arm. Comparative experiments have been carried out and verified the proposed IT method and AIT method in terms of improved maximum achievable stiffness and system transparency performance. It can be concluded that human operators do have the ability and potential to regulate the mechanical impedance of their arms unconsciously and subsequently resist destabilizing factors in haptic systems.

In the future, force fields other than the magnetic force field can be studied for tuning the mechanical impedance of the human arm more effectively. And experiments with a larger number of participants may be carried out to research the dynamic properties of the mechanical impedance of human arms. Moreover, the proposed IT and AIT methods can coexist with passivity-based methods, which is promising for further improving system stability and transparency performance, especially for rendering rigid objects with large stiffness values.

Acknowledgements

This work was partly supported by the National Natural Science Foundation of China Foundation (No. 61773205), the Fundamental Research Funds for the Central Universities (NS2016032, NS2019018, Nanjing University of Aeronautics and Astronautics), and the scholarship from China Scholarship Council (No. 201906835020). The authors gratefully acknowledge the contribution of reviewers' comments.

References

1. X. J. Chen and J. L. Hu, "A review of haptic simulator for oral and maxillofacial surgery based on virtual reality," *Expert Rev Med Devic*. **15**(6), 435–444 (2018).
2. D. H. Kim, Y. Kim, J. S. Park and S. W. Kim, "Virtual reality simulators for endoscopic sinus and skull base surgery: The present and future," *Clin Exp Otorhinolar*. **12**(1), 12–17 (2019).
3. M. H. Abidi, A. M. Al-Ahmari, A. Ahmad, S. Darmoul and W. Ameen, "Semi-immersive virtual turbine engine simulation system," *Int J Turbo Jet Eng*. **35**(2), 149–160 (2018).
4. A. I. Aviles-Rivero, S. M. Alsaleh, J. Philbeck, S. P. Raventos, N. Younes, J. K. Hahn and A. Casals, "Sensory substitution for force feedback recovery: A perception experimental study," ACM T Appl Percept. **15**(3) (2018).
5. J. E. Colgate, P. E. Grafing, M. C. Stanley and G. Schenkel, "Implementation of stiff virtual walls in force-reflecting interfaces," *IEEE Virtual Reality Annual International Symposium*, (1993) pp. 202–208.
6. J. E. Colgate and G. Schenkel, "Passivity of a Class of Sampled-Data Systems - Application to Haptic Interfaces," *Proceedings of the 1994 American Control Conference,* (1994) pp. 3236–3240.
7. J. E. Colgate, M. C. Stanley and J. M. Brown, "Issues in the haptic display of tool use," *Iros '95–1995 Ieee/Rsj International Conference on Intelligent Robots and Systems: Human Robot Interaction and Cooperative Robots, Proceedings*, (1995) pp. 140–145.
8. J. E. Colgate, J. M. Brown and IEEE, "Factors affecting the Z-width of a haptic display," in *1994 Ieee International Conference on Robotics and Automation: Proceedings, Vols 1-4* (Ieee International Conference on Robotics and Automation, Los Alamitos: IEEE, Computer Soc Press (1994) pp. 3205–3210.
9. L. Y. Hu, J. H. Li, X. P. Liu, P. W. Xiong and S. X. He, "The maximum output force controller and its application to a virtual surgery system," *Int J Adv Robot Syst*. **15**(2), 10 (2018).

10. V. Mendez, M. Tavakoli and J. Li, "A method for passivity analysis of multilateral haptic systems," *Adv Robotics*. **28**(18), 1205–1219 (2014).
11. A. Mashayekhi, R. B. Boozarjomehry, A. Nahvi, A. Meghdari and P. Asgari, "Improved passivity criterion in haptic rendering: Influence of Coulomb and viscous friction," *Adv Robotics*. **28**(10), 695–706 (2014).
12. C. Budai, L. L. Kovacs and J. Kovecses, "Combined effect of sampling and coulomb friction on haptic systems dynamics," *J Comput Nonlin Dyn*. **13**(6), 10 (2018).
13. S. Y. Baek, S. Park and J. Ryu, "An enhanced force bounding approach for stable haptic interaction by including friction," *Int J Precis Eng Man*. **18**(6), 813–824 (2017).
14. S. Park, R. Uddin and J. Ryu, "Stiffness-reflecting energy-bounding approach for improving transparency of delayed haptic interaction systems," *Int J Control Autom*. **14**(3), 835–844 (2016).
15. A. Mashayekhi, S. Behbahani, F. Ficuciello and B. Siciliano, "Analytical stability criterion in Haptic Rendering: The Role of Damping," *IEEE-ASME T Mech*. **23**(2), 596–603 (2018).
16. N. Lapanaphan and E. L. J. Bohez, "High impedance actuator fusion: A new concept for a haptic system," *Int J Robot Autom*. **30**(5), 447–457 (2015).
17. A. Jafari, M. Nabeel and J. H. Ryu, "The input-to-state stable (ISS) approach for stabilizing haptic interaction with virtual environments," *IEEE T Robot*. **33**(4), 948–963 (2017).
18. M. Koul, M. Manivannan and S. K. Saha, "Effect of dual-rate sampling on the stability of a haptic interface," *J Intell Robot Syst*. **91**(3–4), 479–491 (2018).
19. Q. V. Dang, L. Vermeiren, A. Dequidt and M. Dambrine, "Experimental study on the stability of an impedance-type force-feedback architecture based on an augmented-state observer for a haptic system under time delay using a LMI approach," *P I Mech Eng I-J Sys*. **230**(1), 58–71 (2016).
20. Y. W. Liu, F. W. Meng, B. W. Guan and S. H. Zhang, "Robust stability analysis based on LMI for haptic interface systems with uncertain delay," *Complexity.* 2018(7), Article ID 9342479, 1–10 (2018).
21. M. Kim and D. Y. Lee, "Multirate haptic rendering using local stiffness matrix for stable and transparent simulation involving interaction with deformable objects," *IEEE T Ind Electron*. **67**(1), 820–828 (2020).
22. A. Campeau-Lecours, M. Otis, P. L. Belzile and C. Gosselin, "A time-domain vibration observer and controller for physical human-robot interaction," *Mechatronics*. **36**, 45–53 (2016).
23. Y. Aydin, O. Tokatli, V. Patoglu and C. Basdogan, "Stable physical human-robot interaction using fractional order admittance control," *IEEE T Haptics*. **11**(3), 464–475 (2018).
24. X. Lu and A. G. Song, "Stable haptic rendering with detailed energy-compensating control," *Comput Graph-UK*. **32**(5), 561–567 (2008).
25. S. Amirkhani, B. Bahadorian, A. Nahvi and A. Chaibakhsh, "Stable haptic rendering in interactive virtual control laboratory," *Intel Serv Robot*. **11**(3), 289–300 (2018).
26. H. B. Li, L. Zhang and K. Kawashima, "Operator dynamics for stability condition in haptic and teleoperation system: A survey," *Int J Med Robot Comp.* **14**(2), 10 (2018)
27. E. Burdet, R. Osu, D. W. Franklin, T. E. Milner and M. Kawato, "The central nervous system stabilizes unstable dynamics by learning optimal impedance," *Nature*. **414**(6862), 446–449 (2001).
28. Q. Bi, C. J. Yang, X. L. Deng and J. C. Fan, "Human finger mechanical impedance modeling: Using multiplicative uncertain model," *P I Mech Eng C-J Mec*. **230**(12), 1978–1986 (2016).
29. H. S. Woo and D. Y. Lee, "Exploitation of the impedance and characteristics of the human arm in the design of haptic interfaces," *IEEE T Ind Electron*. **58**(8), 3221–3233 (2011).
30. A. J. Besa, F. J. Valero, J. L. Suner and J. Carballeira, "Characterisation of the mechanical impedance of the human hand-arm system: The influence of vibration direction, hand-arm posture and muscle tension," *INT J Ind Ergonom*. **37**(3), 225–231 (2007).
31. D. Piovesan, A. Pierobon and F. A. M. Ivaldi, "Critical damping conditions for third order muscle models: Implications for force control," *J Biomech Eng-T ASME*. **135**(10), 8 (2013).
32. M. A. Krutky, R. D. Trumbower and E. J. Perreault, "Influence of environmental stability on the regulation of end-point impedance during the maintenance of arm posture," *J Neurophysiol*. **109**(4), 1045–1054 (2013).
33. M. A. Krutky, V. J. Ravichandran, R. D. Trumbower and E. J. Perreault, "Interactions between limb and environmental mechanics influence stretch reflex sensitivity in the human arm," *J Neurophysiol*. **103**(1), 429–440 (2010).
34. J. Mizrahi, "Mechanical impedance and its relations to motor control, limb dynamics, and motion biomechanics," *J Med Biol Eng*. **35**(1), 1–20 (2015).
35. S. A. M. Dehghan, H. R. Koofigar and M. Ekramian, "An adaptive arm's mechanical impedance estimator for rehabilitation robots without force and acceleration sensors," *Int J Syst Sci.* **49**(13), 2784–2796 (2018).
36. D. Piovesan, M. Kolesnikov, K. Lynch and F. A. Mussa-Ivaldi, "The concurrent control of motion and contact force in the presence of predictable disturbances," *J Mech Robot-Trans ASME*. **11**(6), 14 (2019).
37. A. G. Song, L. Z. Pan, G. Z. Xu and H. J. Li, "Adaptive motion control of arm rehabilitation robot based on impedance identification," *Robotica*. **33**(9), 1795–1812 (2015).
38. L. Xiong, S. Ai-guo and Y. Yong-qiang, "Improved haptic rendering through tuning the mechanical impedance of human arm," *2011 IEEE International Conference on Virtual Environments, Human-Computer Interfaces and Measurement Systems* (2011) pp. 5
39. Z. Hao, X. Chen-xi and L. Xiong, "Influence of Mechanical Impedance of Human Arm on the Stability of Haptic Rendering," *2012 IEEE International Conference on Virtual Environments Human-Computer Interfaces and Measurement Systems (VECIMS)* (2012) pp. 130–134.
40. N. Hogan, "Controlling impedance at the man/machine interface," *Proceedings. 1989 IEEE International Conference on Robotics and Automation (Cat. No.89CH2750-8)*, (1989) pp. 1626–1631.